X-620-66-5

NASA TM X-55362

# $N_2$ TEMPERATURE AND DENSITY DATA FOR THE 150 TO 300 KM REGION AND THEIR IMPLICATIONS


BY

N. W. SPENCER
Goddard Space Flight Center

D. R. TAEUSCH
University of Michigan

G. R. CARIGNAN
University of Michigan





DECEMBER 1965

NASA — GODDARD SPACE FLIGHT CENTER

GREENBELT, MARYLAND

X-620-66-5

# $N_2$ TEMPERATURE AND DENSITY DATA FOR THE 150 TO 300 KM REGION AND THEIR IMPLICATIONS

by
N. W. Spencer
Goddard Space Flight Center

D. R. Taeusch
University of Michigan

G. R. Carignan
University of Michigan

December 1965

GODDARD SPACE FLIGHT CENTER
Greenbelt, Maryland

BLANK PAGE

## ABSTRACT



Measurements of the concentration of $N_2$ in the thermosphere obtained by the Thermosphere Probe, and temperatures derived from the resulting density profiles when compared with similar parameters derived from satellite drag, as represented by current model atmospheres, lead to inconsistencies. Typically, the near daytime maximum and the near nighttime minimum density observed ($2.0 \times 10^9$/cc and $1.2 \times 10^9$ cc at 200 km) and the corresponding temperatures (825° K and 725° K) indicate that the assumption, for model atmosphere purposes, of constant boundary conditions at 120 km should be expanded to reflect, probably, a significant diurnal variation.

BLANK PAGE

CONTENTS

## ILLUSTRATIONS



## TABLES

# $N_2$ TEMPERATURE AND DENSITY DATA FOR THE 150 TO 300 KM REGION AND THEIR IMPLICATIONS

## INTRODUCTION

Study of the orbit decay rates of satellites has led to a large amount of revealing atmospheric structure data which, on the basis of acceptable theoretical considerations, have been used to describe the density, temperature, composition, and other properties of the Earth's neutral particle atmosphere. These important results have appeared in various publications and also have provided constraints and boundary conditions for a number of model atmospheres, of which those of Harris and Priester, 1964, and Jacchia, 1964, are probably the most prominent. Also, investigators using rockets and satellites, and employing "direct" measurement techniques with density gages, which "count" particles under essentially known physical conditions of volume, temperature, collection geometry, etc., at rather specific points in the atmosphere, have provided a much smaller, but an increasing quantity of new data which permit an independent determination of the same atmospheric parameters (Spencer, et al, 1965; Nier, et al, 1964; Newton, et al, 1965). Initial comparisons of these data revealed that density values derived from the drag measurements are higher than density values determined from the gage techniques, by approximately a factor of two. Temperature profiles obtained from the "direct" measurements when compared with drag-derived values also exhibit differences which were not considered significant. However, a recent re-evaluation of the earlier density and temperature data and, in addition, consideration of new data presented in this paper which tend to reinforce earlier tentative conclusions, lead us to conclude that there are significant differences.

We feel that the differences observed have a clear consistency that indicates a systematic difference exists between the results obtained by the two different techniques, and thus suggest either that there are appreciable (unknown) errors in the direct measurement data or that there exists a need for modification or expansion of certain of the assumptions upon which the various model atmospheres, which reflect, largely, the "drag" data, are based. Accordingly, this paper will present the data upon which these comments are based, an evaluation of the errors sustained by the gage techniques, and some supporting discussion of the conclusions drawn.

## EXPERIMENTAL TECHNIQUE

It is well known among vacuum laboratory workers that the measurement of the absolute concentration of a particular gas in an evacuated device to a precision of 25-50 percent poses difficult problems particularly when the total pressure is in the $10^{-6}$ torr region or below. The task is least difficult for chemically inactive gases such as molecular nitrogen, for which reasonably well-understood and reliable procedures exist. Fortunately, the most plentiful constituent of the lower thermosphere is molecular nitrogen This fact, and its chemical stability, thus make it likely that measurements of $N_2$ concentration, using laboratory related devices, will lead to concentration data for this atmospheric constituent in which one can have high confidence. This belief is reinforced by the fact that a relatively satisfactory preflight calibration can be accomplished for this gas, in comparison, for example, to atomic or molecular oxygen, for which only very questionable calibrations can be performed with the present state-of-the-art techniques.

The data to be discussed in this paper, molecular nitrogen concentration and temperature, have been obtained through application of a small omegatron mass spectrometer in an experimental approach which is based largely upon kinetic theory considerations. The experimental technique was discussed in detail in an earlier paper (Spencer, et al, 1965) and thus will only be summarized very briefly here.

An atmospheric composition measurement system (see Figure 1), which has been called the Thermosphere Probe (TP) is arranged to be carried aloft and then ejected into the thermosphere from its launching vehicle (see Figure 2). The TP, which is tumbled intentionally end-over-end after ejection from the rocket, contains the omegatron, all supporting electronic systems, and an appropriate telemetry system for $N_2$ data transmissions to ground stations. Data transmitted from the instrument also includes information relative to its orientation which is essential for satisfactory data analysis, and various additional data such as sensor temperature. A representative telemetry record showing $N_2$ pressure variations occurring in the omegatron chamber as the TP tumbles through the atmosphere is shown in Figure 3.

## RESULTS OF PREVIOUS EXPERIMENTS

The data analyses procedures employed to derive the desired atmospheric $N_2$ density and temperature profiles from the observed omegatron chamber pressure, and other data, have been discussed in detail in the earlier publication. In brief review, the density profile is directly determined from measured

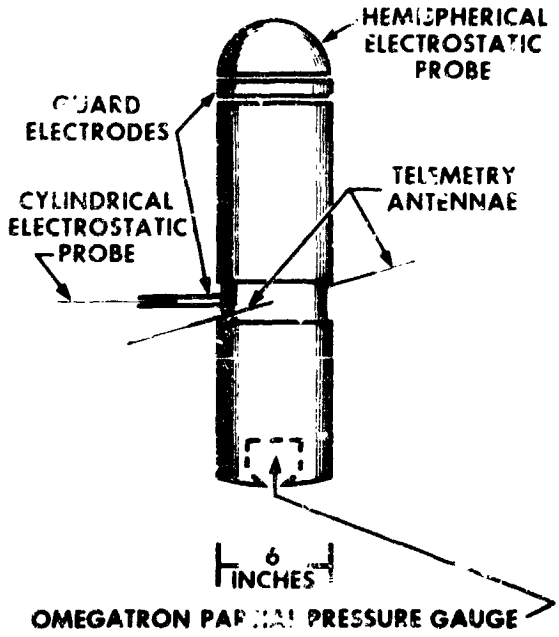


Figure 1. Schematic Representation of Thermosphere Probe (TP)

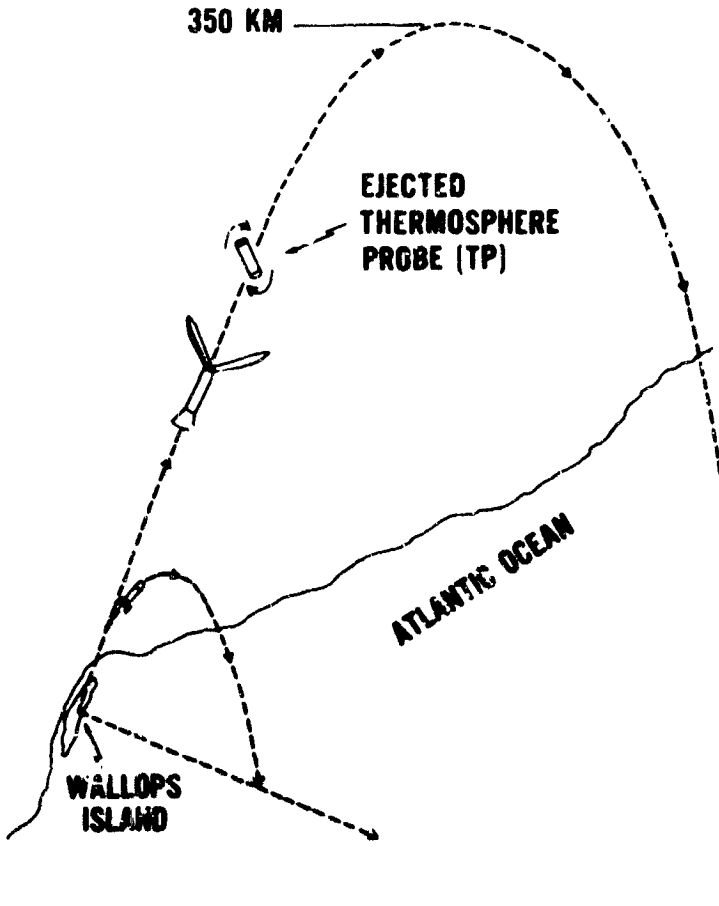


Figure 2. Artist's Representation of Thermosphere Probe Ejection Procedure

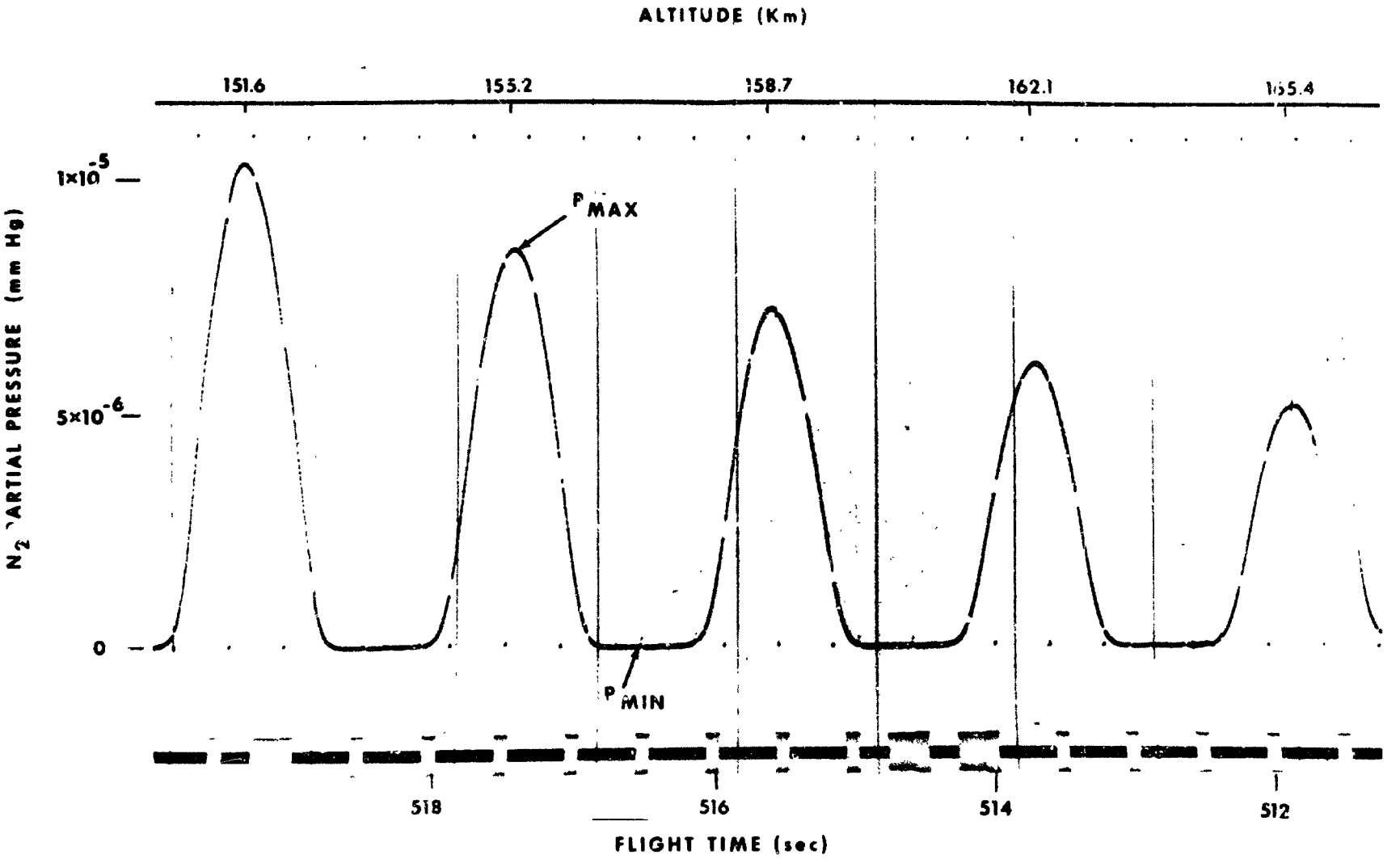


Figure 3. Photograph of Telemetry Record of Typical Omegatron Chamber Pressure

gage density and instrument orientation and velocity. The temperature data are then derived from the density profile, employing scale height considerations. Atmospheric data resulting from these computations are shown in Figures 4 and 5. Harris and Priester 1964 model values most closely approximating solar activity at the times of the experiments are also shown to provide a basis for comparison. A summary of flight statistics of all launchings conducted to date appears in Table I.

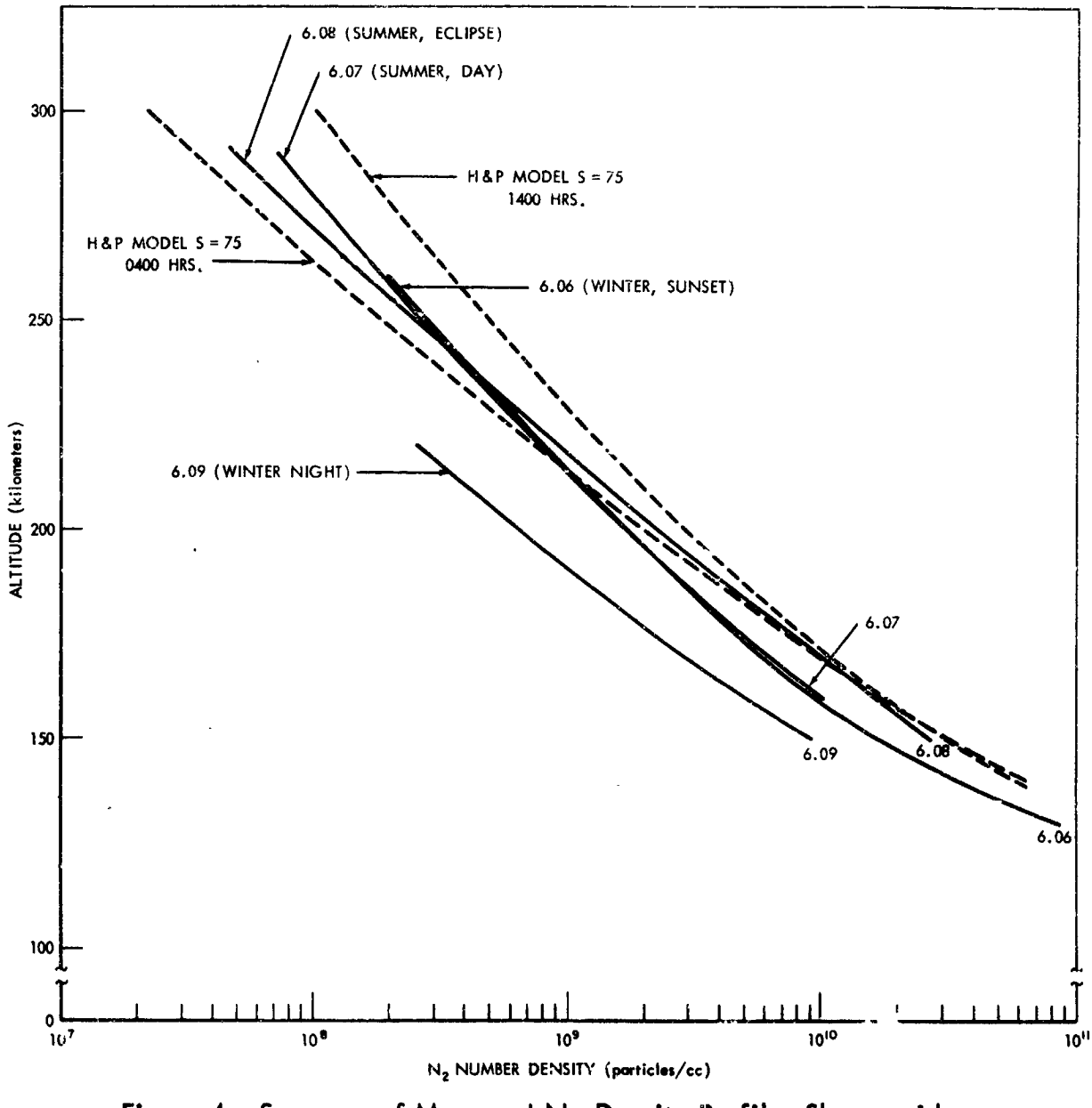


Figure 4. Summary of Measured $N_2$ Density Profiles Shown with Appropriate Model Atmosphere Profiles

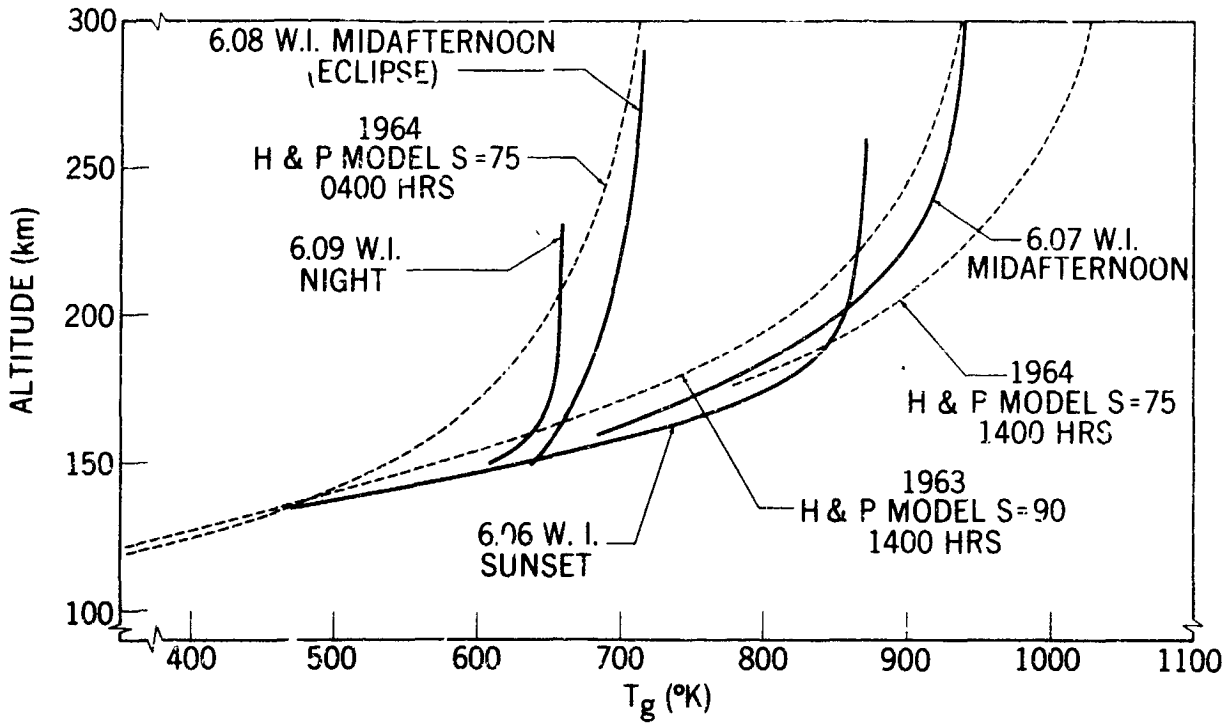


Figure 5. Summary of Early $N_2$ Temperature Profiles with Appropriate Model Atmosphere Profiles

THERMOSPHERE PROBE FLIGHT STATISTICS

| FLIGHT NUMBER | LOCATION | DATE | TIME | | CONDITION | F10.7 $a_p$ |
|---|---|---|---|---|---|---|
| | | | LOCAL | GMT | | |
| 6.06 | Wallops Island | 20 November 62 | 1641 | 2141 | Sunset | 86 4 |
| 6.07 | Wallops Island | 19 April 63 | 1604 | 2104 | Mid-Afternoon (with Explorer 17) | 88 27-38 |
| 6.08 | Wallops Island | 20 July 63 | 1654 | 2154 | Mid-Afternoon (Eclipse) | 77 6 |
| 6.09 | Wallops Island | 28 January 64 | 2209 | 0309 | Nighttime | 78 27 |
| 6.10 | Churchill | 28 July 64 | 1514 | 2114 | Daytime | No Neutral Particle Data |
| 6.11 | Wallops Island | 20 March 65 | 0042 | 0542 | Nighttime | 74 7 |
| 18.01 | Wallops Island | 19 March 65 | 1309 | 1809 | Daytime | 76 5 |
| 18.02* | Churchill | 10 November 65 | 0100 | 0700 | Nighttime | Not Now Available |
| 18.03* | Churchill | 9 November 65 | 1316 | 1916 | Daytime | Not Now Available |

*Data Being Analyzed

Table I

There are a number of comments pertinent to these density and temperature data:

1. All profiles but those labelled NASA 6.08 pertain to the "normal" atmosphere. The 6.08 data were obtained during the July 20, 1963 solar eclipse and will be discussed separately.

2. The general similarity in shape of both the $N_2$ density and temperature data to model profiles confirm gross hydrostatic equilibrium throughout the altitude region. The values of temperature, and the altitudes at which isothermy is observed are in general agreement with accepted concepts; however, the data generally indicate isothermy to significantly lower altitudes than the model, suggesting possibly that there are factors other than conductivity or mass transport that need consideration in model studies. On the other hand, more recent data shown and discussed later in the paper support the gradients depicted by the model.

3. The density data from these earlier flights which are believed to have an absolute accuracy of about 50% or better show a systematically lower density ($N_2$) atmosphere than depicted by the model. In addition, the density values at 150 kms, corresponding to various conditions, show a variation that is inconsistent with the common assumption (for model purposes at least) that the atmosphere at 120 km is essentially invarient.

4. The temperature of the atmosphere is somewhat lower than indicated by the model as illustrated by the NASA 6.07 temperature profile. There are a number of considerations bearing upon this conclusion which will be discussed later in the paper.

5. The profile (6.09) corresponds to winter night, quiet conditions and should reflect nearly minimum solar cycle density for the time (2209 local time) and latitude (Wallops Island 38° N), although the measurement was carried out some six hours prior to the nominal 0400 minimum time. We did have concern, however, over the seemingly low absolute density observed although there are no known aspects of the flight or experiment which lessen our confidence in the data. To confirm the result however, a later experiment was arranged, as will be discussed below.

6. The density of the atmosphere during the solar eclipse of July 20, 1963 was notably different than "normal," as reflected in the 6.08 profile. The 6.07 density profile provides a convenient reference as it was obtained at about the same local time and level of solar activity three

months earlier. The chief difference in conditions was that $a_p$ for the 6.07 experiment was about 30 as compared with a value of about six during the eclipse. One should expect therefore, that the 6.07 density should be greater than 6.08 in the 150 km region, but this was not observed, and the reason may lie in the absolute error of the measurements. It does not appear to be related to semi-annual or seasonal variations, which would favor a lower rather than higher density. Ignoring the difference at the 150 km level (absolute value difference), and noting that the relative accuracy of the data is much better (probably 10% or less) than their absolute accuracy because absolute calibration is not a significant factor, the density at 300 km decreased substantially during the eclipse. This is borne out by the 6.08 temperature profile, which resembles a nearly nighttime exospheric temperature condition. It is important to note, however, that the temperature data derived using scale height considerations depend upon the maintenance of an adequate state of diffusive equilibrium in the atmosphere, and thus the eclipse temperatures may be less accurate than, for example, the 6.07 temperatures.

Assuming, however, that the data are essentially correct, the low temperature reached by the time of eclipse, and the isothermy observed down to about 200 maximum km, reflect the substantial decrease of solar UV and support conclusions of Nicolet (1960) regarding conduction and conduction times. The fact that the density at this time is significantly lower than that considered by Nicolet (nearly a factor of five) indicates that the conclusions he reaches probably apply, at this time in the solar cycle, to significantly lower altitudes (1-2 scale heights). This may explain why the temperatures during the eclipse decreased to values which were to us, surprisingly low.

## NEW EXPERIMENTS

The experiments and data discussed above have shown densities and temperatures systematically lower than the model values chosen for comparison. They have also revealed other aspects, such as relatively large variations of gradients in the 150 - 200 km region. To help resolve this and other questions, several steps have been taken: (a) a pair of experiments to provide a daytime near-maximum $N_2$ density measurement, and a nighttime near-minimum $N_2$ density measurement, have been carried out in a manner to assure nearly identical conditions and with identical instruments, simultaneously calibrated; (b) a re-evaluation of the errors encountered in the experiment has been conducted; and (c) a review of the analysis of the earlier experiment data discussed above has been initiated to reaffirm or reveal the errors sustained.

The results from the two flight experiments are now available and will be discussed, and a preliminary discussion of the error evaluation appears in the appendix. Re-evaluation of the analysis of the earlier data is still underway and will be reported in a subsequent paper.

## DISCUSSION OF NEW DATA: DENSITY

The density data obtained from the day-night pair of experiments is shown in Figure 6, with model values appropriate to existing conditions, linearly

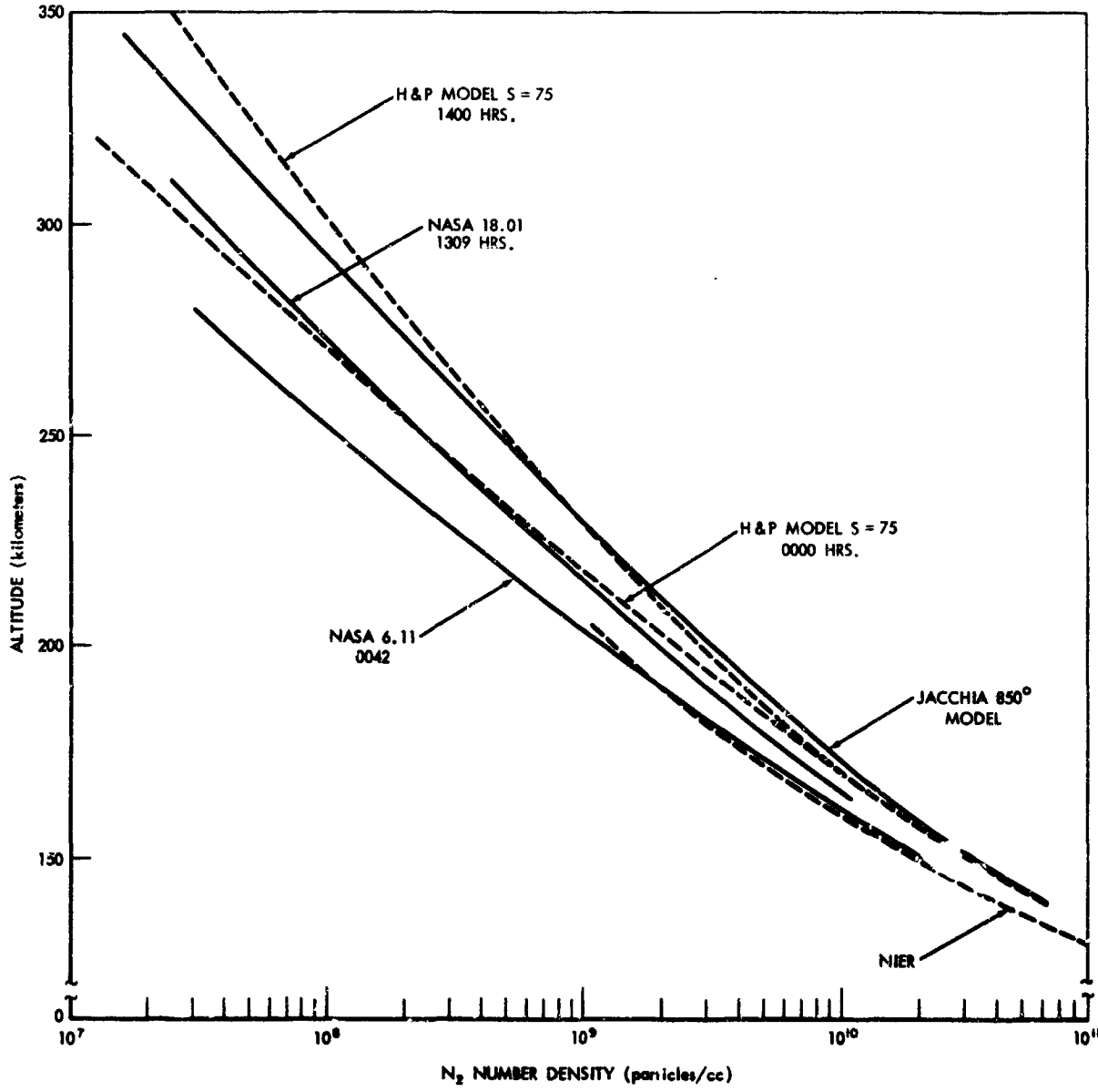


**Figure 6. Recent $N_2$ Density Data Corresponding to Near Daytime Maximum and Near Nighttime Minimum**

extrapolated (the logarithm) to the time of the experiment. The two profiles represent very nearly the maximum and minimum $N_2$ density under conditions of essentially quiet sun (10.7 cm flux $\sim 75 \times 10^{-22}$ w/m$^2$ c/s). The absolute accuracy of the concentrations is believed to be 25% or better and the relative accuracy over the altitude range, and between profiles is believed to be 10% or better. The following comments refer to these data:

1. The data show a lower density $N_2$ atmosphere at 250 km than depicted by the model by a factor of two, with the difference gradually decreasing with decreasing altitude as expected. A reasonable extrapolation of the data for a few km to 150 km shows that the data are lower than the model values by about 40% of the model value at this altitude.

2. The ratio of daytime-to-nighttime density is significantly different than that of the model values. These ratios (model ratio corrected to flight local times) are shown in Figure 7, where, it should be noted, the data ratio curve has been "eyeball"-extrapolated below 170 km. The large difference in ratio seen in the 150-200 km region is of particular interest and will be discussed below.

3. Nier's data (Nier, et al, 1964), although somewhat below the nighttime profile at the lower altitudes, show higher values near 200 km as should be expected (dawn vs nighttime). Conditions at the time of the measurements were made were: time - 0730, location - White Sands, F = 77, $a_p = 16$. There is good agreement with the data presented here.

## DISCUSSION OF NEW DATA: TEMPERATURE

The temperature profiles of the thermosphere derived from the densities shown in Figure 6 are presented in Figure 8, with model atmosphere profiles appropriate to the conditions at the time of the experiments (Harris and Priester, 1964). The model values have also been extrapolated to the local times of the launchings which, as has been noted, correspond very nearly to the times of expected maximum and minimum temperature. Also plotted for comparison are two temperature curves of Jacchia (1964), selected on the basis of exospheric temperatures most closely in agreement with the measured values. Error flags are shown on the derived $N_2$ temperatures, which require a brief discussion. It was stated earlier that the density profiles were believed accurate (relative) to 10% and on an absolute basis to 25%. Temperature calculated using scale height as the basis depends only upon the relative accuracy (the "shape") of the density profiles. The error flags on the temperature data, therefore, reflect the 10% flag on density, with, however, the reservation that

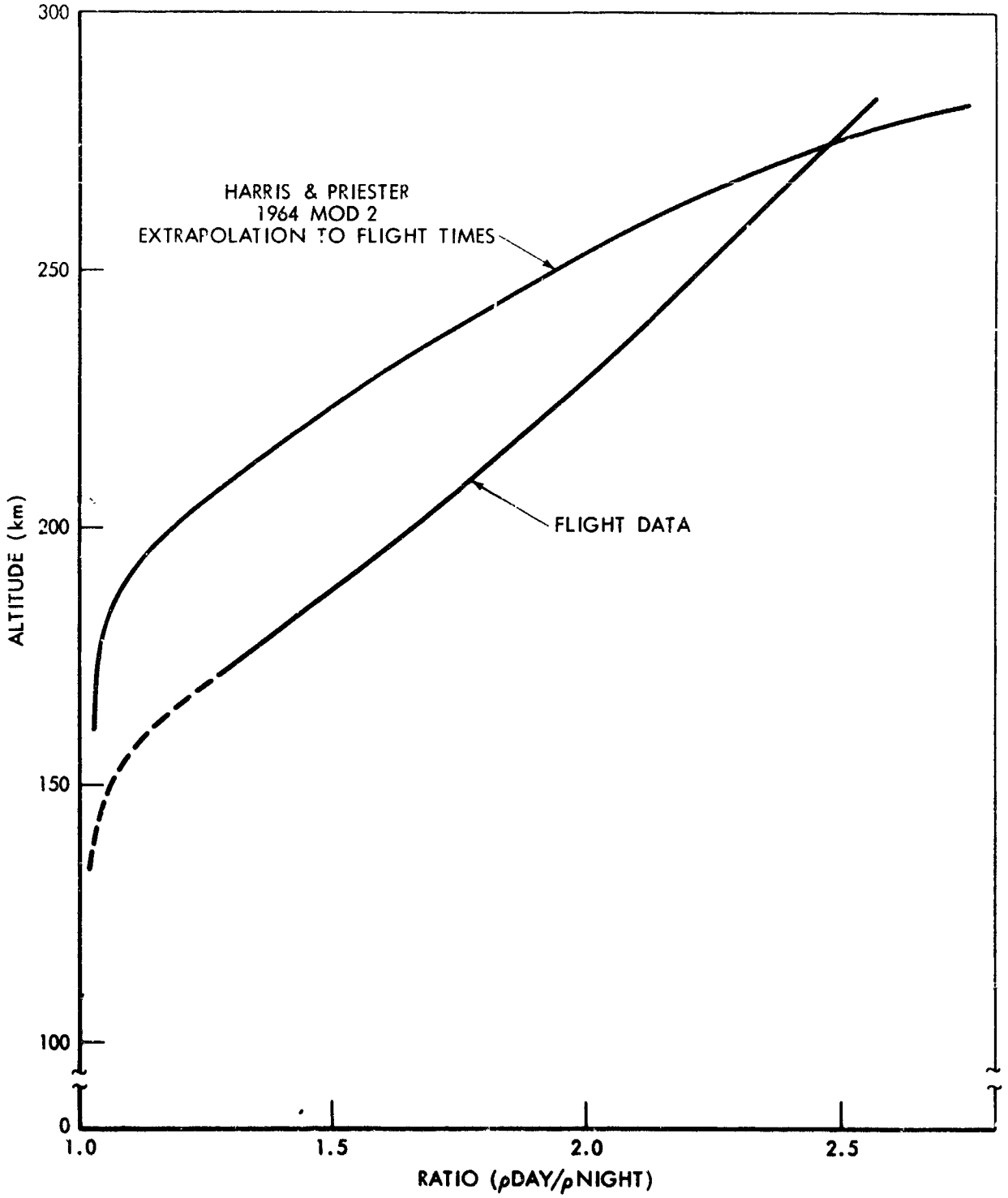


Figure 7. Ratios of Model and Measured Densities Shown in Figure 6

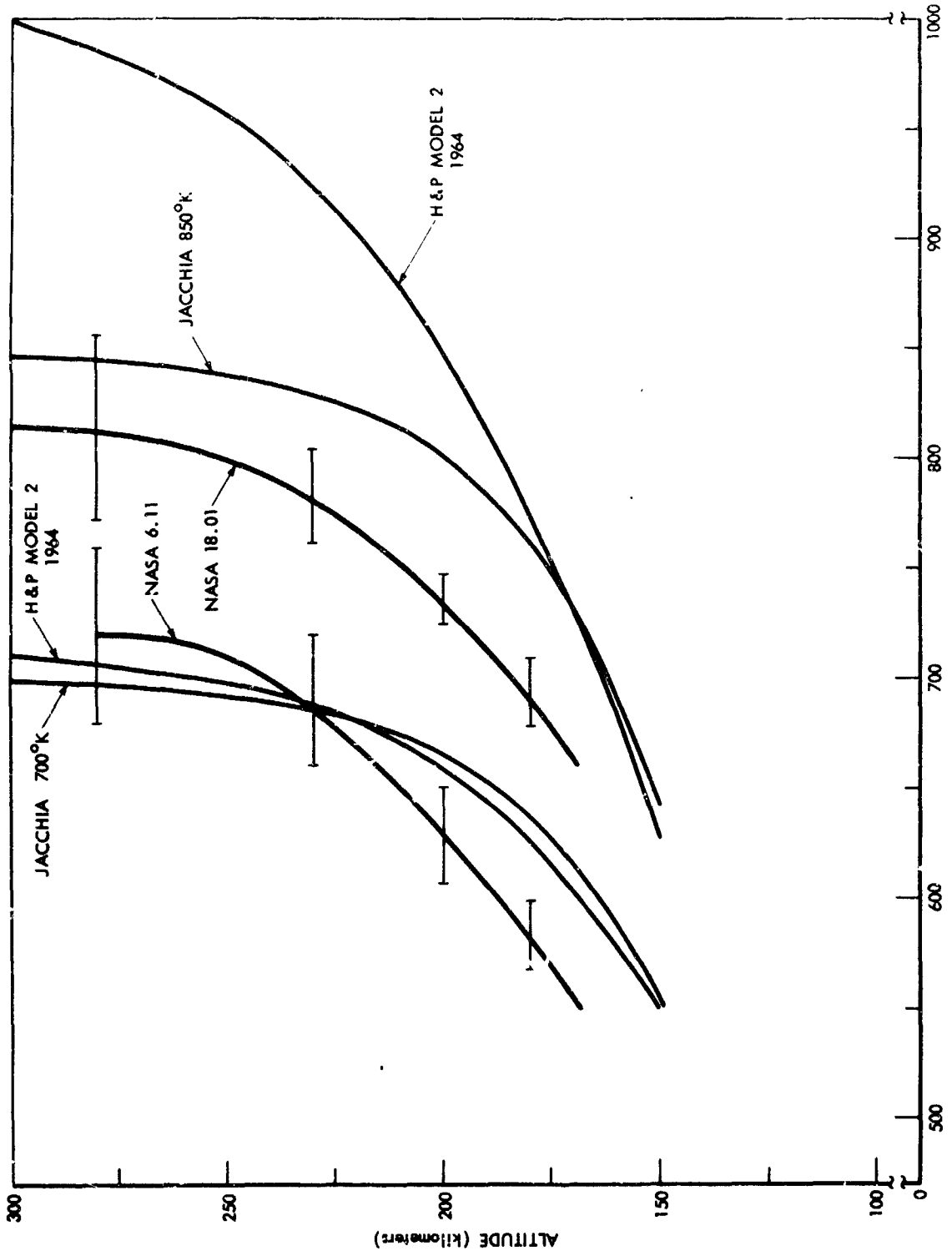


Figure 8. Measured Quiet Sun $N_2$ Temperature Diurnal (Maximum and Minimum) Variation

not all possible curves that could be drawn within the density error flags are acceptable. Clearly, only smoothly varying profiles are acceptable, such as through the maxima, the minima, the mean, or other reasonably acceptable points. In this case, the extremes were determined on the basis of density profiles drawn through the high altitude maximum and low altitude minimum value and conversely, each passing through the medium altitude mean density. These choices should provide extreme temperature profiles. The flags on the temperature curves thus correspond to density curves that reflect the maxima and minima values appropriate to the stated relative accuracy of the density.

There are difficulties, challenges, or dangers in providing a meaningful discussion of the measured temperatures, however, it is probably most fruitful to discuss the temperature profiles in comparison with the model values of Harris and Priester, which for comparison here were chosen on the basis of known solar activity, and the model values of Jacchia which for comparison here were chosen on the basis of measured exospheric temperature. One of the reasons that makes comparisons somewhat uncertain is that the measured values have probable errors which at least permit consideration of improbable gradients. Another reason is that the models must necessarily be considered limited, because not only of probably over-simplified assumptions, but because of the lack of realistic boundary conditions at 120 km. The measured temperatures are, for example, derived from densities which show a diurnal variation of a factor of 1.7 at 200 km which is not compatible with either model. Harris and Priester, for example, as shown in Figure 7, have a ratio of 1.2 at 200 km.

In spite of these difficulties, we feel it is useful to note the apparent differences, as it may lead to a better understanding of the pertinent processes and may contribute to bettering the model representation of the real atmosphere.

1. The measured exospheric diurnal temperature ratio is about 1.15 in contrast to the value 1.20 (determined for time of day and year the experiments were conducted, from Figure 6a, SAO Special Report #150, April 1964, Jacchia) established by a considerable amount of satellite drag data. It must be noted, also, that the error flags permit temperatures which have a ratio of 1.20 or greater. Also, the daytime maximum (measured) is much less than the Harris and Priester model value, although showing isothermy to a comparable altitude. The Jacchia "850° K" curve, on the other hand, is isothermal to an altitude lower by 50 km, as might be expected (less energy absorbed above 250 km).

2. The measured exospheric temperature values are in better agreement with Jacchia temperature data (Figure 8) as deduced from satellite drag using, apparently, a revised Nicolet model. It is interesting to compare

the temperatures with those deduced by Nicolet (1963) for minimum solar activity conditions which occurred in June 1956. See Table II.

| | Day | Night |
|---|---|---|
| Experimental | 825 | 725 |
| Nicolet/1963 | 836 | 629 |

Table II

3. Although the measured nighttime exospheric temperature agrees reasonably well with the model values (Figure 8), the gradients are not in as good agreement, particularly at the 250 km level. In contrast to the nighttime profile, however, is the 6.09 result discussed earlier in the paper, and shown in Figure 5, where isothermy is observed at a considerably lower altitude. No solar or magnetic activity effects are known to account for the difference, and no explanation for the difference is apparent at this time, unless it is due to variable and unknown conditions below 120 km.

4. In considering the measured day-night profiles, one concludes that there is an incompatibility in respect to gradients. For example, the nighttime gradient at some altitudes is quite high in comparison with the corresponding daytime gradient. It should be noted, however, that the insensitivity of the density profile to changes in temperature in this region (hence, the "large" temperature error flags) works against the establishment of meaningful gradient detail. The magnitudes of the two profiles, however, are significant and can be supported. Since a large diurnal density change is observed at 200 km, in which we have considerable confidence and it is not accompanied by a substantial increase in the temperature at 200 km (Harris and Priester model requires over 200° K for only a 20% density increase) some other effect must be determined. It seems to us, therefore, that the best explanation is an increase in the density (and/or temperature) above the mesopause (near or below 120 km), an effect not incorporated in the models. Mass transport horizontally may also be a possible explanation, although Harris and Priester (1964) have tentatively concluded that it is not significant.

## SUMMARY AND CONCLUSIONS

New measurements of the $N_2$ density of the thermosphere corresponding to nearly maximum and minimum of the diurnal variation, have been obtained under quiet sun and low magnetic activity conditions. The density data have been interpreted in terms of the neutral particle temperature.

The results permit the following conclusions:

1. The density variation observed near 300 km is equivalent to that depicted by the Harris and Priester 1964 model (~2.5) but greatly exceeds that indicated by the model at 200 km.

2. The diurnal exospheric temperature variation is considerably less than that indicated by the same model.

3. These two factors (1), (2) are not consistent with present model considerations, and in particular, probably require reconsideration of the constant boundary values at 120 km, as both a density and temperature increase in the region below and near 120 km could explain the data.

4. The measured exospheric temperatures (ignoring error flags) generally are in agreement with the satellite-drag determined temperatures of Jacchia.

5. Improved measurement accuracy is required to establish meaningful details of the temperature gradient in the 200 km region.

6. Measured $N_2$ densities in the thermosphere are systematically lower than satellite-drag determined densities. A factor of two is observed at 250 km.

## ACKNOWLEDGMENT

The authors acknowledge the contributions of the many individuals who participated in the research program which yielded the results reported. At the University of Michigan, H. B. Niemann who supervised the design, construction, preparation and calibration of the omegatron, and J. Maurer who supervised the construction, testing and many of the tasks involved in launching of the Thermosphere Probe, are especially acknowledged. George Newton and his associate, David Pelz at Goddard Space Flight Center, contributed to the program through participation in gage calibration and through much valuable discussion of the data. Finally, the authors express thanks for the excellent support provided by the Goddard Space Flight Center Sounding Rocket Branch and the Wallops Island Rocket Range in carrying out the rocket launchings.

## REFERENCES


1. Nicolet, M., "Structure of the Thermosphere," Planetary and Space Sciences, Vol. 5, pp. 1-32, 1961.

2. Harris, I. and W. Priester, "The Upper Atmosphere in the Range from 120 to 800 km," GSFC, NASA, 1964.

3. Jacchia, L. G., "Static Diffusion Models of the Upper Atmosphere with Empirical Temperature Profiles," Smithsonian Inst. Astrophysical Observatory, Special Report #170, 1964.

4. Spencer, N. W., L. H. Brace, G. R. Carignan, D. R. Taeusch, H. Niemann, "Electron and Molecular Nitrogen Temperature and Density in the Thermosphere," Journal of Geophysical Research, Vol. 70, No. 11, pp. 2665-2698, June 1965.

5. Jacchia, L. G., "The Temperature Above the Thermosphere," Smithsonian Inst. Astrophysical Observatory, Special Report #150, 1964.

6. Nier, A. O., J. H. Hoffman, C. Y. Johnson, J. C. Holmes, "Neutral Composition of the Atmosphere in the 100 to 200 Kilometer Range," Journal of Geophysical Research, Vol. 69, No. 5, March 1964.

7. Nicolet, M., "Solar Radio Flux and Thermosphere Temperature," Journal of Geophysical Research, Vol. 68, November 1963.

8. Newton, G., R. Horowitz, W. Priester, "Atmospheric Density and Temperature Variations from the Explorer XVII Satellite and a Further Comparison with Satellite Drag," Planetary and Space Sciences, Vol. 13, pp. 599-616, 1965.

9. Taeusch, D. R., G. R. Carignan, H. B. Niemann, A. F. Nagy, "The Thermosphere Probe Experiment," Scientific Report No. 1 (07065-1-S), Office of Research Administration, Ann Arbor, March 1965.

BLANK PAGE

Appendix

## ERROR DISCUSSION

The data presented have been reduced from telemetry records similar to that shown in Figure 3. The deflection versus time outputs are read using standard techniques and are reduced to gage number density, wall temperature, etc., using pre-flight calibration of the various instruments. The ambient number density is obtained using the equation:

$$n_a = \frac{\Delta n_i \; U_i}{2\sqrt{\pi} \; V \cos \alpha} \tag{1}$$

where

$n_a$ = $N_2$ ambient number density

$\Delta n_i$ = measured maximum-minus-minimum $N_2$ number density

$U_i$ = $\sqrt{2KT_i/m}$ = most probably thermal speed of particles inside measuring chamber

$V$ = speed of TP with respect to earth

$\alpha$ = minimum angle between velocity vector of TP and plane of tumble.

The basic assumptions in the derivation are (a) the measured gas has a Maxwellian distribution of velocities, both inside and outside the measuring chambers; (b) the particles inside the chamber are fully accommodated to the chamber wall temperature, (c) the atmosphere rotates with the earth, and (d) certain implicit assumptions concerning gage geometry and homogeneity which will be discussed in a later section.

As can be seen from Equation (1), the uncertainty in the calculated ambient number density depends upon the uncertainty in the measured quantities $\Delta n_i$, $U_i$, $V$ and $\alpha$ approximately in the following manner:

$$\frac{\delta n_a}{n_a} = \frac{\delta(\Delta n_i)}{\Delta n_i} + \frac{\delta U_i}{U_i} - \frac{\delta V}{V} + \tan \alpha \delta \alpha \qquad (2)$$

The gage sensitivity used to obtain $\Delta n_i$ is determined from a vacuum calibration of the sensor. In general, in the calibration several Bayard-Alpert ionization gages are used as secondary standards after having been calibrated against a McLeod gage. Several calibrations of the omegatron are performed and self-consistency between the BA gages and the omegatron calibration is carefully established. In the case of NASA 18.01 and NASA 6.11, the two omegatrons were calibrated simultaneously on the same system. All of the other data from other flights presented were also obtained from omegatrons which were calibrated on the same vacuum system with the same BA gage secondary standards. As a result, it is believed that the relative accuracy of the calibration data is better than ±10 per cent. For NASA 18.01 and NASA 6.11 the relative accuracy of the calibration data is probably better than ±5 per cent. An evaluation of the factors known to effect the validity of the absolute calibration leads to the conclusion that the absolute accuracy is ±25 per cent.

$U_i$, the most probable thermal speed of the particles within the measuring chamber, is calculated from the measured chamber wall temperature, which is measured by a thermistor and is believed known to be better than ±2 per cent. Since $U_i$ involves the square root of the temperature, the resulting error contribution in Equation (2) is on the order of ±1 per cent.

The TP velocity, V; angle of attack, $\alpha$; and the basic independent variable, altitude, are determined using trajectory data obtained from radar. These data were obtained, at Wallops Island, Virginia, from the FPS-16 and FPQ-6 radars. The FPS-16 specification accuracy is ±5 yards in range and ±0.1 mil in azimuth and elevation. The FPQ-6 specification accuracy is ±5 yards in range and ±0.05 mil in azimuth and elevation. A theoretical trajectory is fitted to the radar data, and considered adequate when the downleg low altitude information agrees better than ±0.5 km. The resulting velocity data are better than ±1 per cent. Since the TP and rocket motor separate at approximately 4 feet per second and it is uncertain which portion the radar is tracking, ±0.5 km is adopted as the uncertainty in altitude at approximately 120 km altitude on the downleg portion of the trajectory. This is equivalent to approximately ±0.25 km at peak altitudes and a very small error for upleg data. This uncertainty in altitude implies a ±5 per cent maximum uncertainty in the density versus altitude profile for the low altitude downleg data.

The angle of attack data are obtained through an optical technique using the method described by Taeusch, Carignan, Niemann and Nagy (1965). This

method requires two measured inputs to determine an angular momentum vector. The angular momentum vector and the velocity vector (from radar data) are then used to determine the angle of attack. The total effect of errors in the three measured quantities varies greatly with geometry and is best considered for each individual case. A worst case analysis for the data presented herein yields a possible error in $\alpha$ of approximately 5°. The effect of an uncertainty in $\alpha$ on the computed density, depends on $\alpha$ (Equation 2). Figure 9 shows this dependency. For a stable rocket, $\alpha$ minimum is near zero at ejection, and typically less than 20° during most of the ascending leg. The angle of attack versus altitude for NASA 18.01 is plotted in Figure 10 for illustrative purposes. For an uncertainty in $\alpha$ of ±5° at an $\alpha$ of 20°, the resultant uncertainty in density is ±3 per cent. A plot of the effect of $\delta\alpha$ on $\delta n_\alpha/n_\alpha$ is shown in Figure 9.

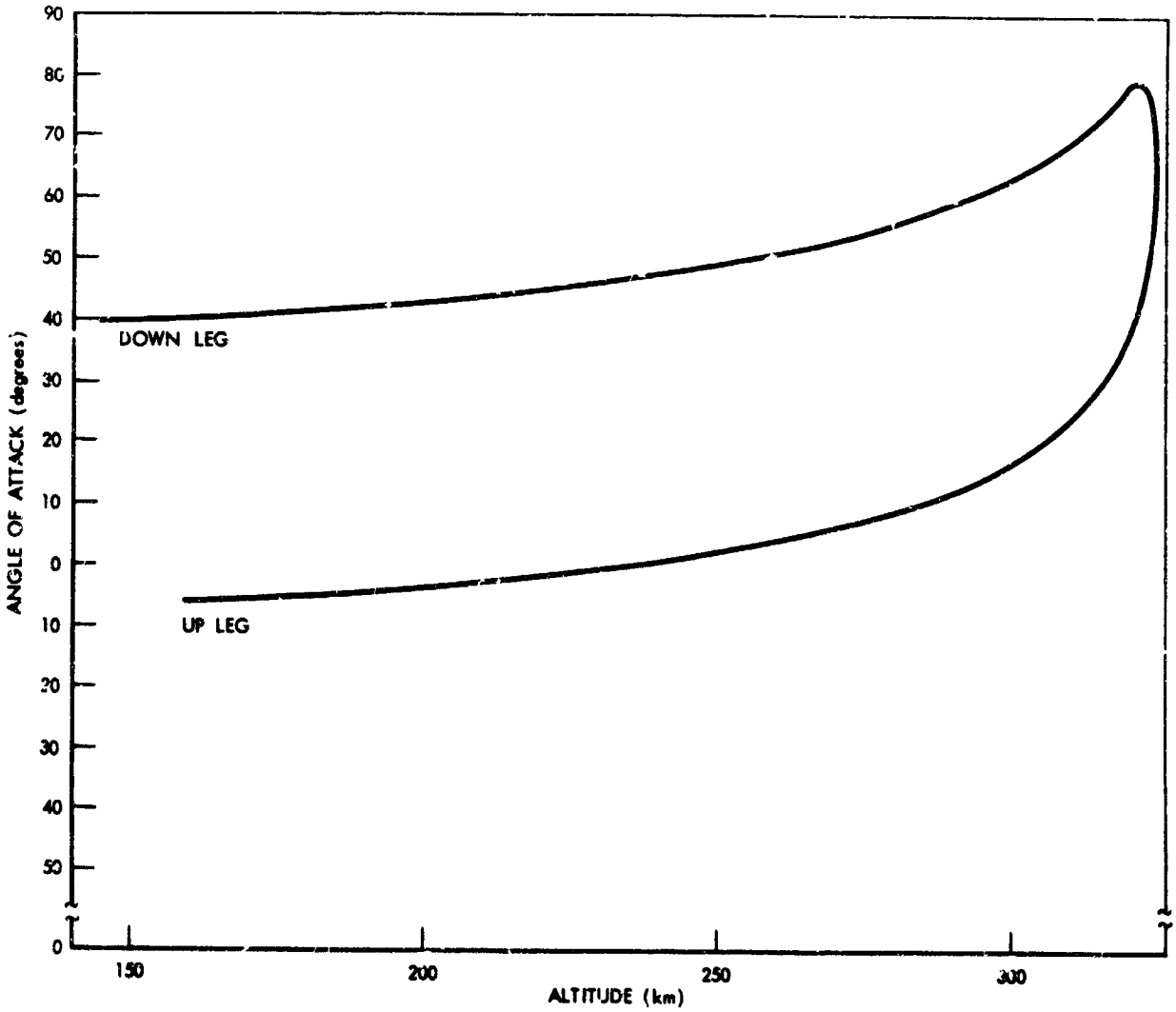


Figure 9. History of the Angle Between the TP Tumble Plane and the Velocity Vector for Flight NASA 18.01

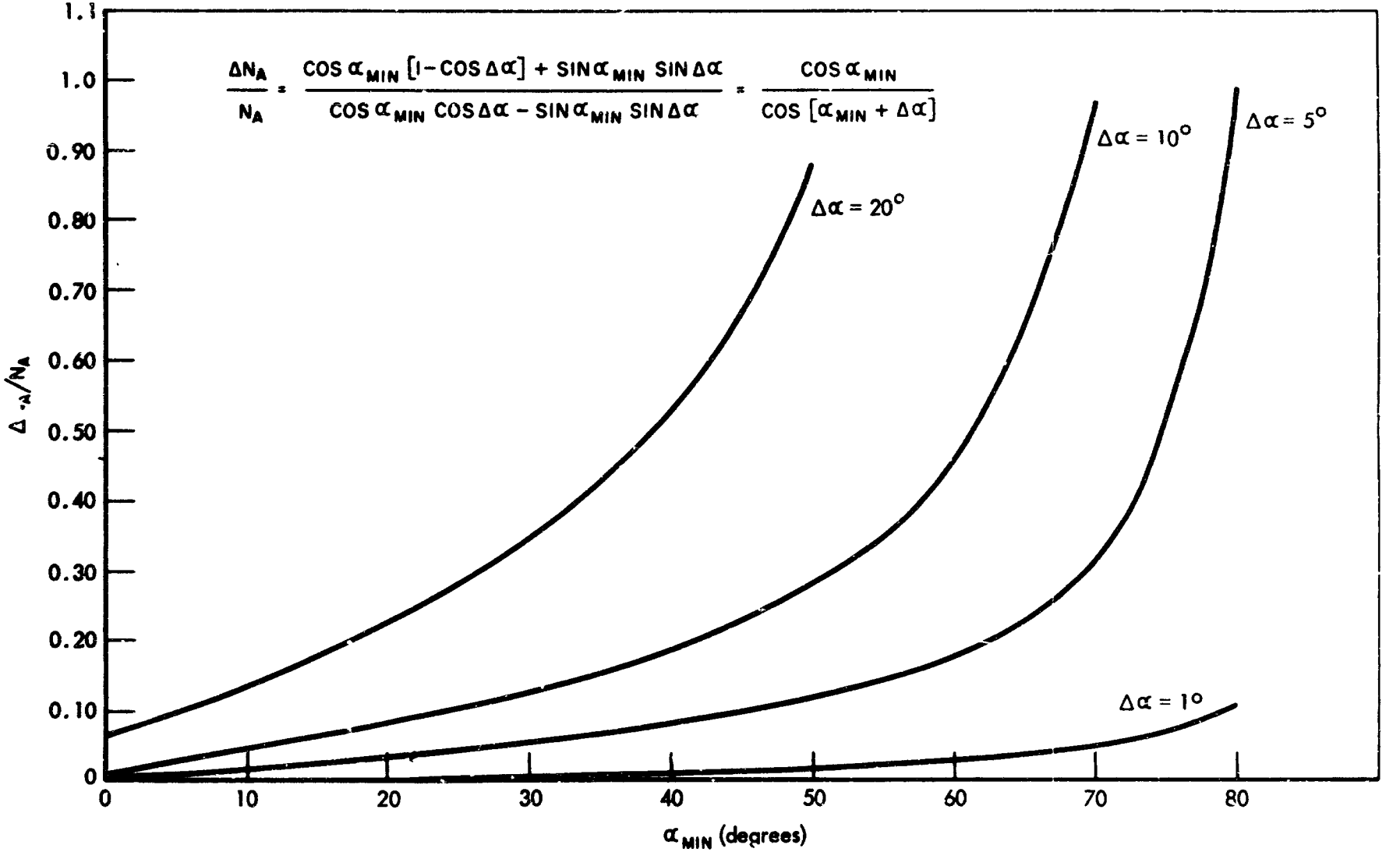


Figure 10. Error in Ambient Density Due to Error in α Minimum, for Various α

Telemetry and reading errors which contribute to the uncertainty in $\Delta n_i$ and $U_i$ are on the order of ±2 per cent. Therefore, we see in Equation (2) that, for relative considerations:

$$\frac{\delta(\Delta n_i)}{\Delta n_i} \simeq \begin{cases} \pm 10\% \text{ relative calibration} \\ \pm 2\% \text{ telemetry and reading} \\ \pm 25\% \text{ absolute calibration} \end{cases}$$

$$\frac{\delta U_i}{U_i} \simeq \begin{cases} \pm 1\% \text{ absolute calibration} \\ \pm 2\% \text{ telemetry and reading} \end{cases}$$

$$\frac{\delta V}{V} \simeq \pm 1\%$$

$$\tan \alpha \delta \alpha \simeq \pm 3\%$$

or

$$\frac{\delta(\Delta n_i)}{\Delta n_i} \simeq \pm 10.2\% \text{ RMS relative} \simeq \pm 25.1\% \text{ RMS absolute}$$

$$\frac{\delta U_i}{U_i} \simeq \pm 2.2\% \text{ RMS absolute}$$

and

$$\frac{\delta n_a}{n_a} \simeq \pm 10.9\% \text{ RMS relative} \simeq \pm 25.4\% \text{ RMS absolute}$$

Finally, it is appropriate to discuss briefly a correction that is made necessary by imperfections in gage geometry. As stated previously, the derivation of Equation (1) required certain assumptions concerning gage geometry and "homogeneity" of the particles within the gage. One major assumption made in the use of Equation (1) is that the orifice diameter is small compared to the mean free path and the chamber dimensions. Since, however, this would, if strictly true, result in poor conductance between the chamber and atmosphere, a chamber pressure time response problem would exist. Rather than create this problem for the measurement, the gage orifice is made large enough to allow quick response to the density changes due to tumble and altitude changes. The output varies from that theoretically expected during a tumble cycle.

Therefore, empirical correction factors are determined from the data during those times of low minimum $\alpha$, as shown in Figure 11. These corrections are then applied to the data obtained when the minimum $\alpha$ is high. Figure 12 shows the correction factors for various $s_0$'s for flight NASA 18.01. The effect of this correction factor on the data uncertainty is a function of the minimum angle of attack and the ability to determine the factor adequately from flight data. It has been determined that the maximum correction to be made to the data is of the order of 18%, and the correction is determinable from flight data. A negligible relative error is believed and assumed to result, and accordingly, is not considered in the error calculation.

The normalization of the measured and theoretical curves at $\alpha = 0$ implies that the relationship expressed by Equation (1) is correct at that point. The validity of this assumption is now being studied and the results will be reported at a later time.

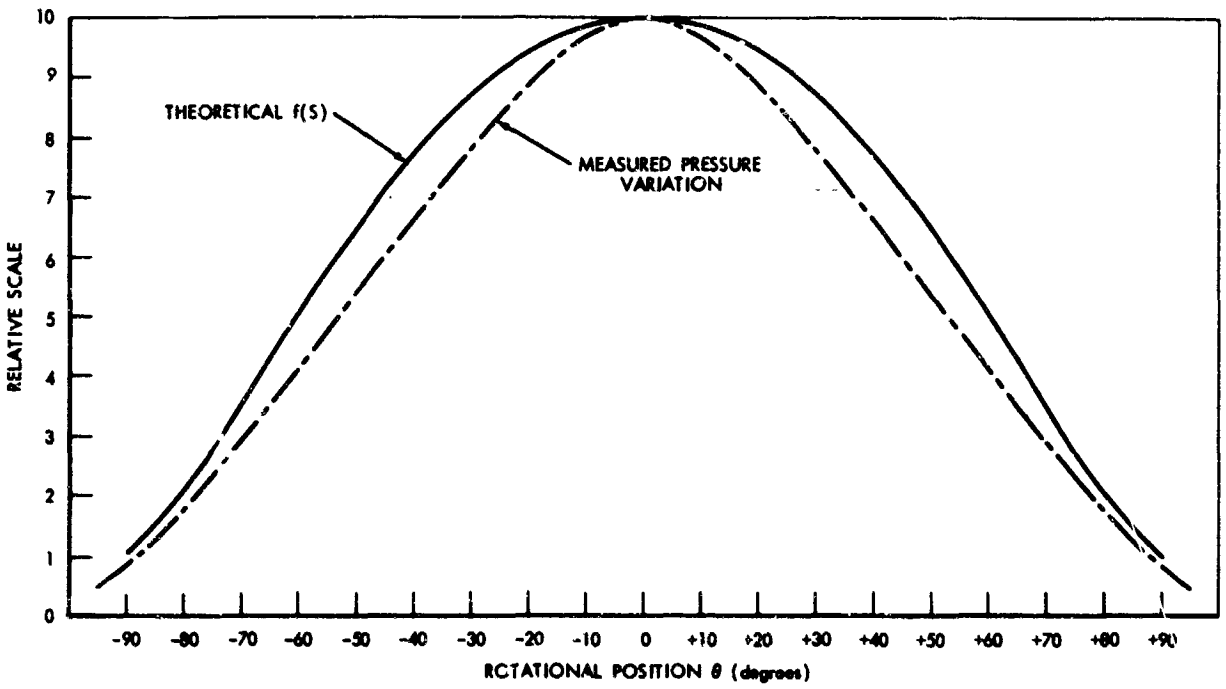


LEGEND

| | |
|---|---|
| NASA 18.01 | TEMPERATURE = 675°K |
| · = DATA POINTS | $\alpha_{min} = 5.314°$ |
| TIME OF PEAK = 95.75 SEC | $S_0 = 2.79$ |
| ALTITUDE = 171.4 KM | $S_{MAX} = S_0 \cos \alpha_{min} = 2.78$ |

**Figure 11. Theoretical and Experimental Variation of Pressure Due to f(s)**

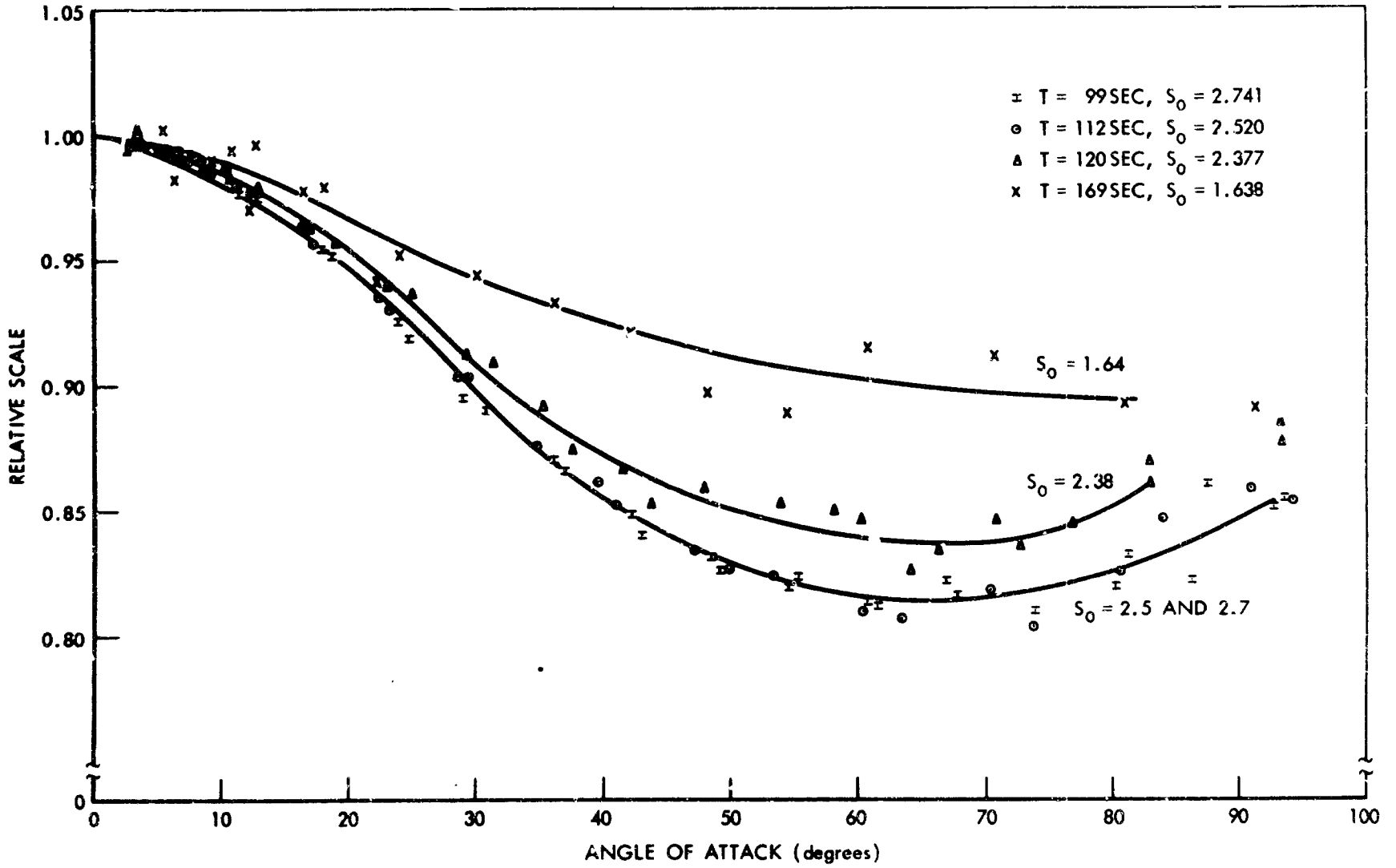


Figure 12. Experimental Values of f(s) as a Function of Angle of Attack and s